ILASS–Europe 2022, 31th Conference on Liquid Atomization and Spray Systems, 6-8 September 2022, Virtual, Israell

Effect of Dissolved Carbon Dioxide on Cavitation Inception and its Development in a Circular Orifice

Sina Safaei*[1], Carsten Mehring[2]
[1] Institute of Mechanical Process Engineering, Stuttgart, Germany
[2] Institute of Mechanical Process Engineering, Stuttgart, Germany
*Corresponding author: sina.safaei@imvt.uni-stuttgart.de

Abstract
Prediction of cavitation inception is an important topic for the prevention of cavitation damage as well as its promotion and control in various process applications. Liquids that experience cavitation may contain dissolved gases, which affects cavitation inception and the faith of cavitation bubbles. In this work, an experimental setup is developed for the preparation of water containing a controlled amount of dissolved carbon dioxide and in order to investigate the effect of the dissolved gas on cavitation inception and cavitation development in a sharp-edged orifice, similar to that previously analysed by Nurick in context of unlike-impinging-doublet liquid injectors [1]. Cavitation inception points are determined for different dissolved gas concentration levels by measuring wall static pressures just downstream of the orifice contraction. Flow visualization is performed in order to observe the onset of cavitation bubble formation at the inception point as well as the development of the cavitation zone with further increase in upstream pressure. An increase in the amount of dissolved carbon dioxide is found to increase the cavitation number at which onset of cavitation occurs. For high concentrations of dissolved carbon dioxide gas cavitation, i.e. the desorption or evolution of dissolved gas from the liquid phase, occurs parallel to vapour cavitation and can be distinguished from the latter by visual inspection. Volume flow rate measurements are performed to enable the determination of discharge coefficients for the investigated cases. CFD analyses employing Singhal's full cavitation model [2] (thereby accounting for both vapour and gas cavitation) are conducted for the investigated orifice geometry. Discharge coefficients obtained from the numerical solutions are in good agreement with experimental values although slightly higher in the cavitating case. The earlier onset of fluid cavitation (i.e. cavitation inception at higher cavitation numbers) due to the existence of dissolved carbon dioxide, was not predicted accurately by the employed cavitation model.

Keywords
Cavitation number, Cavitation inception, Outgassing, dissolved carbon dioxide, discharge coefficient

1. Experimental System

1.1 Experimental Setup – Water preparation cycle

In order to investigate the effect of dissolved gases on cavitation inception and its evolution, the amount of non-condensable dissolved gases should be adjustable and controllable in the experimental set-up. In an upfront water preparation cycle, water is pumped from the bottom of a tank to a membrane contactor, where the absorption and desorption of gases in or out of the liquid takes place. The contactor contains inlet and outlet ports for water as well as for the gas. For degasification of water a vacuum pump is connected to the corresponding gas port of the contactor while the “sweep” gas port remains closed. In order to dissolve non-condensable gases in water the contactor is used in sweep mode. For this purpose, the “sweep” gas is introduced to the contactor at the corresponding gas port, while the vacuum gas port remains closed. At suitable time intervals water samples are taken and guided to the measurement chamber, where the gas sensors measure the dissolved gas concentration. Dissolved oxygen is measured by an optical oxygen sensor, nitrogen and carbon dioxide concentrations are measured by two thermal conductivity gas sensors. To reach higher gas concentrations an air compressor is utilized to increase the pressure level within the system. In this work we use carbon dioxide as sweep gas because of its higher solubility in comparison to nitrogen and oxygen. Water with three different levels of dissolved carbon dioxide concentration are prepared for the measurements. The table in Figure 1 summarizes the dissolved gas concentrations for the three investigated cases.

Gas type	Concentration [ppm]		
	GC1	GC2	GC3
Carbon dioxide	0	318	707
Oxygen	0.85	1.09	0.42
Nitrogen	2.03	2.41	1.30

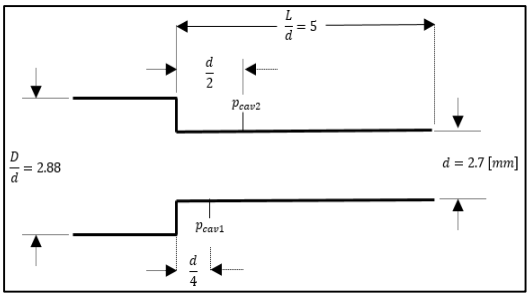

FIGURE 1 LEFT: IN WATER DISSOLVED GAS CONCENTRATIONS FOR THE 3 INVESTIGATED CASES. RIGHT: GEOMETRY OF THE SHARP-EDGE ZYLINDRICAL ORIFICE AND POSITIONS OF CAVITY PRESSURE TAPS 1 AND 2.

1.2 Experimental Setup – Cavitation inception in sharp-edged orifice

Cavitation inception is investigated for water flowing through a sharp-edged orifice. The test section was drilled and polished out of PMMA for flow visualization purposes. Figure 1 shows the dimensions of the orifice including the positions of pressure taps. The orifice is a scaled-down version of the Lucite orifice employed by Nurick [1]. The scale-down was necessary due to flow rate limitations based on available water tank volume and the required testing time to assure steady-state conditions for each measurement. For cavity pressure measurements two pressure taps have been precision drilled and are located at d/2 and d/4 distance from the sharp-edged contraction across which the cylindrical cross section reduces from diameter D to d. In the employed flow system set-up, water flow is maintained by pressure build up in the water tank using an air compressor providing tank pressures of up to 10 bar. The orifice inlet pressure must be precisely regulated in order to resolve the inception point. This has been accomplished by using a back-pressure regulator. Water mass flow rate is measured upstream of the orifice by a magnetic mass flow meter. The experiments and measurements were conducted for orifice inlet pressures between 0.96 bar to 3 bar. High pressure build up in the tank (10 bar) just behind the pressure valve guarantees that during the experiments, the orifice inlet pressure remains constant. No free or evolved gas was observed at the orifice inlet within our experiments.

1.3 Basic definitions

The likelihood of a flow in an orifice to develop cavitation can be characterized by the cavitation number, CN, which is commonly defined as $CN = (p_1 - p_v)/(p_1 - p_2)$ where p_1, p_2 are the pressures upstream and downstream of the orifice and p_v denotes the (equilibrium) vapor pressure of the liquid. The dimensionless cavity pressures at the position of the pressure taps shown in Figure 1 can be defined as $P_{cav1,2} = p_{cav1,2}/(p_1 - p_2)$. The actual mass flow rate through an orifice can be characterized by the discharge coefficient which is defined as $C_d = \dot{m}_a/\dot{m}_t$, where $\dot{m}_a$ and $\dot{m}_t$ represent the actual and the theoretical mass flow rates, respectively. The theoretical mass flow rate describes the mass flow in the absence of any losses. In our case, it can be written as the mass flow rate through a straight tube of diameter d with the same pressure conditions as for the orifice case and without any frictional losses, i.e., $\dot{m}_t = \left(\frac{\pi d^2}{4}\right)\sqrt{2\rho_l(p_1 - p_2)}$, where ρ_l is liquid water density. Various expressions can be found in the literature for determining the discharge coefficient. A vital consideration in this context is the presence or absence of cavitation in the nozzle. Since the orifice geometry investigated here conforms to hat considered by Nurick [1], we use Nurick's analytical expressions for cavitating flow in nozzles as reference.

2. Results

2.1 Comparison of cavity pressure with Nurick experiment

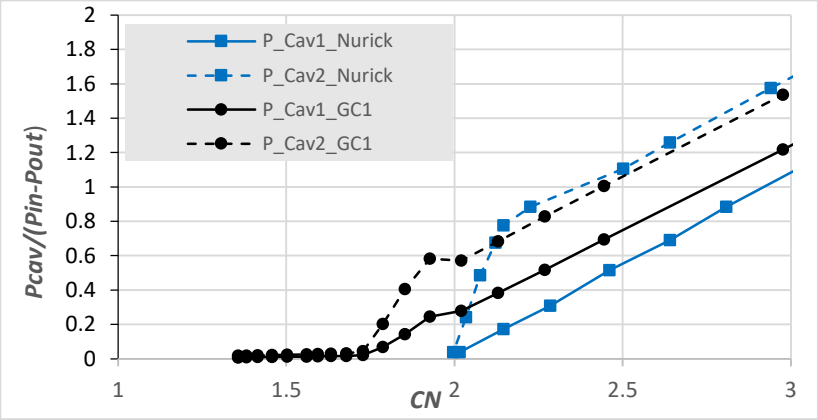

FIGURE 2. COMPARISON OF DIMENSIONLESS CAVITY PRESSURES AT TAP POSITIONS 1 AND 2 (ACCORDING TO FIG. 1) WITH NURICK [1]

Figure 2 illustrates the dimensionless cavity pressures measured at tap positions 1 and 2 (as specified in Figure 1) dependent on cavitation number, CN, for water with aeration level GC1 (i.e., no dissolved CO_2) in comparison to Nuricks investigation [1]. It can be observed that in Nuricks experiment the cavity pressure reaches the vapor pressure at higher cavitation numbers. The deviation from Nurick results is likely due to a difference in the value of entrance roundness and its relation to the orifice diameter(s). As already reported by Nurick, the roundness of the sharp-edged entrance region has a significant influence on cavity pressure and consequently on cavitation inception [1]. In addition to entrance roundness, anomalies along the edge of the contraction caused by drilling and polishing the orifice can affect the flow through the contraction and consequently cavity pressures as well. These effects are stronger for cavity pressure at tap 1, which is located closer to the contraction. It should be noted in this

context, that our orifice geometry is approximately a factor 3 smaller than Nurick's Lucite orifice.

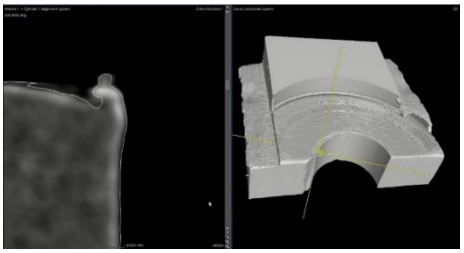

FIGURE 3. RIGHT: CT-SCAN OF ORIFICE REGION AFTER TESTING WITH ANOMALIES ALONG THE EDGE OF THE CONTRACTION. LEFT: ZOOM-IN OF ANOMALY IDENTIFIED BY THE YELLOW CROSSHAIR (RIGHT).

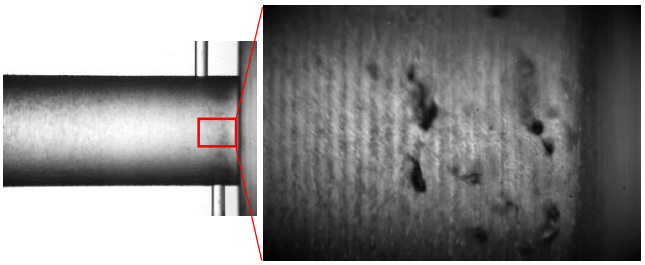

FIGURE 4. FUZZY REGION JUST DOWNSTREAM OF SHARP-EDGE ORFICE AT CAVITATION INCEPTION.

Figure 3 shows topological anomalies along the edge of the orifice captured by a CT-Scan of the orifice region after testing had been concluded. Aside from geometric scaling effects there are other scaling effects which need to be considered to assure similarity between hydrodynamically "similar" cavitating flows [3] and which might have contributed to the observed differences between the present results and those reported by Nurick. A detailed explanation of these effects is beyond the scope of this text.

2.2 Influence of dissolved gases on cavitation inception

In the work presented by Nurick [1] cavitation inception was characterized by the formation of a fuzzy region near contraction. Flow visualization at inception using a high-speed camera shows that the fuzzy region consists of tiny vapor bubbles which disappear further downstream due to pressure recovery. Figure 4 illustrates vapor bubbles generated at inception. The images were captured at a frame rate of 100k [fps]. Figure 5 depicts the change of cavity pressures as function of cavitation number for the three CO2 aeration levels GC1, GC2 and GC3 listed in Table 1. As already noted by Nurick [1] the instance of cavitation inception is recognized by a plateau in the plot for cavity pressure at tap 1. Cavitation numbers at inception points are 1.93, 2.02 and 2.14 for aeration levels GC1, GC2 and GC3, respectively. Visual observations of inception (via appearance of the prescribed fuzzy region) confirm these values as shown in Figure 5. It can be deduced that an increase in dissolved gas concentration leads to higher cavitation numbers at inception. Considering now the flow images at cavitation number CN=2.03 (inserted in Figure 5) shows that for aeration level GC1, i.e., no CO2 dissolved, no cavitation occurs. This is in agreement with the information from the cavity pressure curves, according to which inception in this case occurs at CN=1.94. Note that the size of the cavitation cloud for aeration level GC3 is bigger than that for aeration level GC2 at that same cavitation number even though the cavity pressures do not vary. This seems to indicate that the potential of cavitation generation improves with an increase in dissolved gas concentration. From the images we also note that, for case GC3 there is a notably higher amount of CO2 gas bubbles being released into the access port of pressure tap 1 than in the GC2 case. It is noted, that in the present case outgassing occurs parallel to vapor cavitation. Onset of outgassing or gas cavitation is governed by the threshold or equilibirum pressure given by the sum of the liquid's vapor pressure and CO2 gas-phase partial pressure; the latter being determined (under equilibrium conditions) by Henry's law and the amount of dissolved gas molar fraction in the liquid. In contrast vapor cavitation occurs if the local fluid pressure drops below the critical pressure given by the sum of liquid vapor pressure augmented by the maximum principal component of the strain-rate tensor [3] and including the effects of turbulent fluctuations. As water containing noticeable amounts of dissolved gases passes through the

flow contraction the static pressure drops below the prescribed equilibrium pressure leading to gas desorption. Vapor bubbles also appearing in the low pressure zone due to cavitation will collapse as soon as they migrate to the areas, where the fluid pressure has recovered. In contrast to vapor bubbles, gas bubble formation and dissolution occurs by diffusion. Once formed, these bubbles will persist due to the large characteristic time associated with this process in comparison to those of the other relevant processes. Accordingly, gas bubbles will predominantly found further downstream of the contraction zone or in the recirculation regions next to the vena contract. Evidence of the latter is given by the gas bubbles detected in the pressure tap access ports, especially at high dissolved CO2 concentrations.

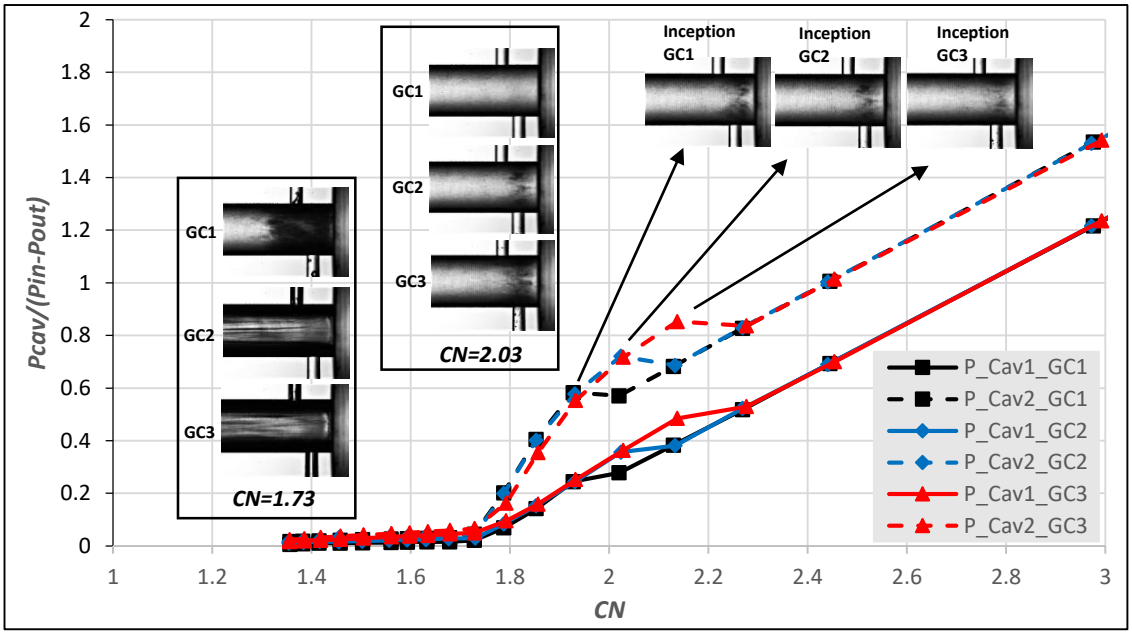

FIGURE 5. CAVITATION INCEPTION AND EVOLUTION AS FUNCTION OF DISSOLVED CO2 CONTENT. SHOWN ARE PRESSURE VALUES AT TAP POSITIONS 1 AND 2 (SEE FIG.2) AS FUNCTION OF CAVITATION NUMBER. AN INCREASE IN DISSOLVED GAS CONCENTRATION LEADS TO CAVITATION ONSET AT HIGHER CAVITATION NUMBERS

2.3 Measurements of discharge coefficient and comparison with numerical simulations

Various predictive models have been developed to predict cavitation and outgassing phenomena in the framework of CFD simulations. Here we employ the so-called “full cavitation model” by Singhal [2] which was one of the first to consider both processes and which is still in widespread use in industry today. The model considers three phases, namely liquid water together with the dissolved (non-condensable) gas phase, the vapor-phase of the liquid (in our case water) and the gaseous phase of the non-condensable gas, in our case carbon dioxide. The three phases are considered as a homogeneous mixture without slip velocity between the phases, i.e., the three phases share the same velocity field. For a detailed explanation of the model the reader is referred to Singhal [2]. The model is available in the commercial flow solver CFX v19.1 by ANSYS Inc. See also Lifante and Frank [5]. The model has been successfully applied to numerous industrial applications and for various liquids and gases, see for example also Mehring [4]. For the simulations of the present flow configuration only carbon dioxide is considered as dissolved non-condensable gas. The Henry constant for carbon dioxide was chosen to be $1.6 * 10^8\ [pa]$. The presence of dissolved oxygen and nitrogen was neglected. Figure 6 shows a comparison of the orifice discharge coefficients C_d obtained from the present experimental results, predicted by our CFD simulation results and predicted by Nurick’s correlation for this orifice geometry [1]. We first note, that while the

amount of dissolved CO2 changes the cavitation number CN at which cavitation first occurs (see discussion above), it does not notably change the variation of discharge coefficient with CN. Also, experimental results are in excellent agreement with Nurick's correlation. Simulation results for the discharge coefficient are in good agreement with experimental results in the non-cavitating case (high CN-values) and also agree well with Nurick's correlation in the full cavitation zone (CN < 1,3). The simulations predict cavitation onset at smaller cavitation numbers resulting in an overprediction of discharge coefficient in the respective range of cavitation numbers. Similar to our experimental observations, the simulations do not show a dependence of dissolved CO2 on the variation of discharge coefficient with CN.

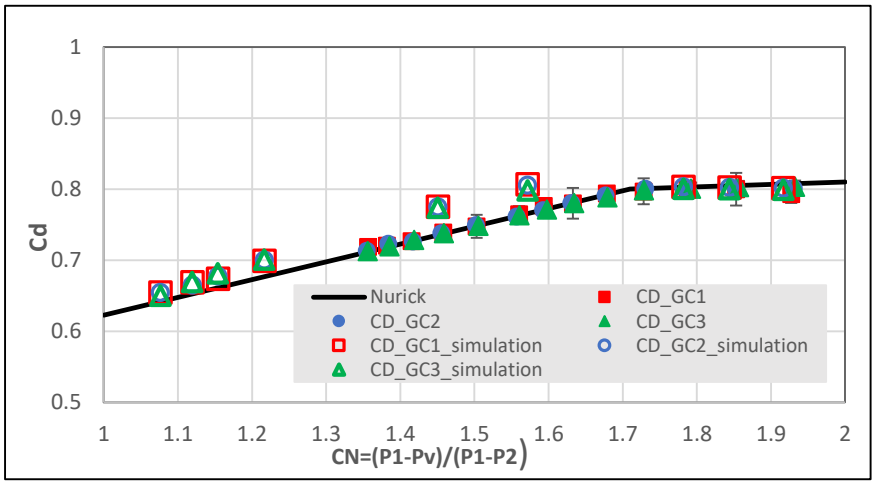

FIGURE 6. DISCHARGE COEFFICIENT AS FUNCTION OF CAVITATION NUMBER BASED ON EXPERIMENTAL RESULTS, CORRELATION BY NURICK [1] AND CFD SIMULATION RESULTS BASED ON THE FULL CAVITATION MODEL BY SINGHAL [2].

3. Summary

In order to investigate the effect of dissolved gases on cavitation inception and its evolution in a sharp-edged orifice, water with three concentrations of dissolved CO2 was prepared. The cavitation inception point was detected via measuring wall static pressures and visual observations. It is found, that an increase in dissolved CO2 concentration leads to higher cavitation numbers at which inception occurs. Outgassing, i.e. the desorption of dissolved gas from the liquid phase, was found to occur in parallel to vapour cavitation for the investigated cases. CFD analyses based on Singhal's full cavitation model predict values for discharge coefficient that are in good agreement with experimental data, No dependence of dissolved CO2 concentration on the variation of discharge coefficient with cavitation number was observed.

References

[1] Nurick, W. H., 1976, Orifice cavitation and its effect on spray mixing. ASME J. Fluids Eng., 98, pp. 681–687.

[2] Singhal, A. K., Athavale, M. M., Li, H., Jiang, Y., 2002, Mathematical basis and validation of the full cavitation model. ASME. J. Fluids Eng., 124(3), pp. 617–624.

[3] S. Martynov, D. Mason, M.R. Heikal, S.S. Sazhin, M. Gorokhovski, Modelling of cavitation flow in a nozzle and its effect on spray development, Annals of the Assembly for International Heat Transfer Conference 13, 2006, 16.70

[4] Mehring, C., 2013, Liquid-fuel ejector pump under multi-phase flow conditions, 25th European Conference on Liquid Atomization and Spray Systems.

[5] Lifante, C., Frank, T., 2008, Investigation of higher order pressure fluctuations and its influence on ship stern, taking into account cavitation at the propeller blades. Otterfing, Germany: ANSYS Germany GmbH.